Supporting Information

Kim et al. 10.1073/pnas.1110406108

SI Materials and Methods

Plant Materials and Growth Conditions. RNAi-C1 (1), which targets the four cytosolic *Arabidopsis HSP90* genes, was crossed into a *CCR2:LUC*$^{+}$ reporter background (2). F1 seedlings exhibiting kanamycin (RNAi-C1, 50 μg/mL) and gentamycin (*CCR2:LUC*$^{+}$, 50 μg/mL) resistance were selected, and antibiotic resistant F2 progeny were scored phenotypically at the adult stage for bushy growth, an indicator of HSP90 reduction (1). *TOC1-YFP* (*TMG*) (3) and the *PRR:PRRn –GFP* transformants have been described previously (4). *gi-2* (5), *gi-201* (6), *GI:GI-TAP* (7), and *35S:GI-OX* (8) have been described previously. All plant materials were grown under 12 h white fluorescent light (50–60 μmol m^{-2} s^{-1})/ 12 h dark cycles (LD) for 8–12 d on MS media (Murashige and Skoog; GIBCO) plates with 3% sucrose and 0.8% agar, as previously described (9).

HSP90.1, .2, and .4 artificial microRNA (amiRNA) plasmids were generated using pAmiR-HSP90.1 (CSHL_078887), pAmiR-HSP90.2 (CSHL_079907), and pAmiR-HSP90.4 (CSHL_079899), which were obtained from ABRC. HSP90.1–4 and HSP90.3 amiRNA plasmids were generated using Web MicroRNA Designer 2 (http://wmd2.weigelworld.org). Primers for HSP90.1–4 and HSP90–3 amiRNA were specified using Web MicroRNA Designer 3 oligo design algorithm initiated using the RS300 vector sequence and the following core amiRNA sequences of the target genes (or common gene family) to generate each specific amiRNA (HSP90.1–4: TTAGAAAGCAGCGTACTCTTC; HSP90.3: TCTCCCGAAAGTGTTGGGGTC). Overlapping PCR and subsequent subcloning was performed as described previously (10). The amiRNA primers used are described in Table S5.

Seedlings for luminescence rhythm analysis were grown and period estimates determined as previously described (9) unless otherwise noted.

For period determination experiments using geldanamycin (GDA), seedlings were grown on MS agar media in LD for 5–7 d and transferred at ZT 0.5 to 24-well tissue culture plates (BD Falcon) filled with water containing 0.3 mM luciferin (Biotium) and either 0.02% DMSO (vehicle control) or 2 μM GDA. Plates were then transferred to constant red light (17 μmol m^{-2} s^{-1}) for the duration of the experiment and imaged every 2 h. For protein expression experiments, 7- to 10-d-old LD-grown seedlings (MS agar media) were harvested at ZT 4, and remaining seedlings were then incubated in 0.05% DMSO (vehicle control) or 5 μM GDA in water-filled Petri dishes (60 × 15 mm) and harvested at the indicated times while a second addition of 5 μM GDA (or DMSO) was administered at ZT 14.

Protein Analysis. Protein extraction and immunoblot detections were performed as described previously (8). For immunoprecipitation of ZTL and coimmunoprecipitation of HSP90, anti-ZTL polyclonal antibody was preincubated with protein A agarose (Invitrogen) at 4 °C, after which protein extracts were incubated for 1 h with gentle rotation. Immune complexes were washed three times, resuspended in SDS/PAGE sample buffer, briefly heated, and subjected to SDS/PAGE and following immunoblotting. For HSP90 immunobloting, protein was transferred to PVDF membrane (Bio-Rad) and incubated with the affinity-purified anti-HSP90 antibody (1:1,000) for 4 h at room temperature or overnight at 4 °C. The membranes were developed using peroxidase-conjugated secondary antibody (1:3,000–5,000) (GE Healthcare) by enhanced chemiluminescence (SuperSignal West Pico Chemiluminescent substrate; Pierce Biotechnology).

Ten-day-old *Arabidopsis* whole seedlings grown under 12 h light/12 h dark condition on MS plates or *Nicotiana benthamiana* leaves 3 d after agroinfiltration were subjected to in vivo protein cross-linking as previously described (11).

The ORF of *Arabidopsis* Hsp90.2 (AtHsp90.2, At5g56030) and ZTL (At5g57360) was introduced into pET28a and pMal c2X to produce recombinant protein with 6xHis tag and maltose-binding protein (MBP-ZTL), respectively. The plasmids were transformed into *Escherichia coli* BL21 (DE3) pLysS for protein expression. *E. coli* cells harboring the plasmid were grown at 30 °C until OD600 approached 0.8. Protein expression was induced by the addition of 0.5 mM (His-AtHsp90.2) and 1 mM (MBP-ZTL) isoprophyl-1-thio-β-D-galactopyranoside for another 3 h at 37 °C, and the cells then were harvested by centrifugation. The harvested cells were resuspended in PBS and disrupted by sonication. After centrifugation, the resulting supernatant of His-AtHsp90.2 and MBP-ZTL was applied onto a Ni-NTA Sepharose CL-6B affinity column (Peptron) and Amylose resin (New England Biolabs), respectively. AtHsp90.2 protein was eluted by thrombin digestion (16 h/4 °C) and MBP-ZTL eluted using 10 mM maltose in PBS. For buffer exchanges, the eluted proteins were subjected to gel filtration chromatography with elution buffer (50 mM Hepes, pH 7.5) by using an ÄKTA fast performance liquid chromatography system with a prepacked Superdex 200 HR 10/30 column (Amersham). Protein concentration was determined using a Bio-Rad protein assay. The chaperone activity of AtHsp90.2 was assayed by measuring its capacity to suppress aggregation of MBP-ZTL. Purified recombinant MBP-ZTL using affinity column chromatography was incubated with 10 mM DTT at room temperature for 1 h and then purified by PD-10 column (GE Healthcare) to remove remaining DTT in buffer. Reduced ZTL was confirmed by SDS/PAGE, and the fourth elution of MBP-ZTL (1 μM) was applied in the absence or presence of AtHsp90.2 with various molar ratios for holdase chaperone assay under denaturing conditions (26.6 mM Gn·HCl and 45 °C) for 20 min by measuring the absorbance at 340 nm using a Beckman DU-800 spectrophotometer (Beckman Coulter) attached to a thermostatic cell holder assembly. BSA was used as a negative control.

PCR Techniques. RT-PCR was performed using conditions and sequences as previously described (4). Ubiquitin 10 (*UBQ10*, AT4g05320) was used as a control for semiquantitative RT-PCR analysis. For RT-PCR analysis using protoplasts, 800 μL of protoplasts were used for transfection using 200 μg of amiR-control, amiR-HSP90.1–4, or mixture of amiR-HSP90.1, 90.2, 90.3, 90.4 (50 μg per each amiRNA). Protoplasts were harvested at ZT 4 after 19 h incubation in the entraining chamber after transfection. RNA extraction and real-time quantitative PCR (qPCR) was performed as previously described (10). RT-PCR primers used are described in Table S5.

Luminescence Assay. Protoplast isolation and DNA transfection was performed as previously described with minor modifications (10). Briefly, protoplasts were isolated at ZT 4 from 25-d-old *Arabidopsis* rosette leaves grown in 12 h light/12 h dark. Extracted protoplasts were resuspended in W5 solution [154 mM NaCl, 125 mM $CaCl_2$, 5 mM KCl, 1.5 mM Mes-KOH (pH 5.7), and 5 mM glucose], at a concentration of 1.5×10^5 mL^{-1}. DNA transfections were performed by mixing 200 μL protoplasts, 55 μg of amiRNA plasmids, and 16 μg of *CCA1:luciferase* reporter plasmids with PEG solution (40% PEG-4000, 200 mM mannitol, and 100 mM $Ca[NO_3]_2$). Transfected proplasts (3×10^4)

were transferred into a 96-well microplate and incubated from ZT 9 under constant red light condition. Image collection and quantitation were performed as described previously with minor modifications (12). Period lengths are reported as variance-weighted period ± SEM, which were estimated using bioluminescence data obtained from 36 to 144 h under constant conditions.

Yeast Two-Hybrid Interaction Assay. The protein-coding sequence of *Arabidopsis* HSP90.2 and ZTL were cloned into the donor vector (pDONR-221) and subsequently moved into the bait (pDEST32) and prey (pDEST22) vectors using the recombination-based Gateway cloning system (Invitrogen) according to the manufacturer's instructions. The primer sets are 5′-AAAAAGCAGGCTTCATGGCGGACGCTGAAACCTT-3′ and 5′-AGAAAGCTGGGTCGTCGACTTCCTCCATCTTGCT-3′ for HSP90.2, and 5′-AAAAAGCAGGCTTCATGGAGTGGGACAGTGGTTC-3′ and 5′-AGAAAGCTGGGTCCGTGAGATAGCTCGCTAGTGA-3′ for ZTL. Sets of constructs including empty vectors were cotransformed into a pJ694A yeast strain. Yeast transformants were selected on glucose-based synthetic minimal medium (SD; 0.67% yeast nitrogen base, 2% glucose, amino acids dropout solution) deficient in tryptophan and leucine either in the absence or presence of histidine. Quantitative yeast two-hybrid interaction assays (β-galactosidase assay) were performed using ortho-nitrophenyl-β-D-galacpyranoside as a substrate according to published protocols (8).

1. Sangster TA, et al. (2007) Phenotypic diversity and altered environmental plasticity in *Arabidopsis thaliana* with reduced Hsp90 levels. *PLoS ONE* 2:e648.
2. Schultz TF, Kiyosue T, Yanovsky M, Wada M, Kay SA (2001) A role for LKP2 in the circadian clock of *Arabidopsis*. *Plant Cell* 13:2659–2670.
3. Más P, Kim WY, Somers DE, Kay SA (2003) Targeted degradation of TOC1 by ZTL modulates circadian function in *Arabidopsis thaliana*. *Nature* 426:567–570.
4. Fujiwara S, et al. (2008) Post-translational regulation of the *Arabidopsis* circadian clock through selective proteolysis and phosphorylation of pseudo-response regulator proteins. *J Biol Chem* 283:23073–23083.
5. Fowler S, et al. (1999) GIGANTEA: A circadian clock-controlled gene that regulates photoperiodic flowering in *Arabidopsis* and encodes a protein with several possible membrane-spanning domains. *EMBO J* 18:4679–4688.
6. Martin-Tryon EL, Kreps JA, Harmer SL (2007) GIGANTEA acts in blue light signaling and has biochemically separable roles in circadian clock and flowering time regulation. *Plant Physiol* 143:473–486.
7. David KM, Armbruster U, Tama N, Putterill J (2006) Arabidopsis GIGANTEA protein is post-transcriptionally regulated by light and dark. *FEBS Lett* 580:1193–1197.
8. Kim WY, et al. (2007) ZEITLUPE is a circadian photoreceptor stabilized by GIGANTEA in blue light. *Nature* 449:356–360.
9. Somers DE, Kim WY, Geng R (2004) The F-box protein ZEITLUPE confers dosage-dependent control on the circadian clock, photomorphogenesis, and flowering time. *Plant Cell* 16:769–782.
10. Kim J, Somers DE (2010) Rapid assessment of gene function in the circadian clock using artificial microRNA in *Arabidopsis* mesophyll protoplasts. *Plant Physiol* 154:611–621.
11. Rohila JS, Chen M, Cerny R, Fromm ME (2004) Improved tandem affinity purification tag and methods for isolation of protein heterocomplexes from plants. *Plant J* 38:172–181.
12. Kim J, Kim Y, Yeom M, Kim JH, Nam HG (2008) FIONA1 is essential for regulating period length in the *Arabidopsis* circadian clock. *Plant Cell* 20:307–319.

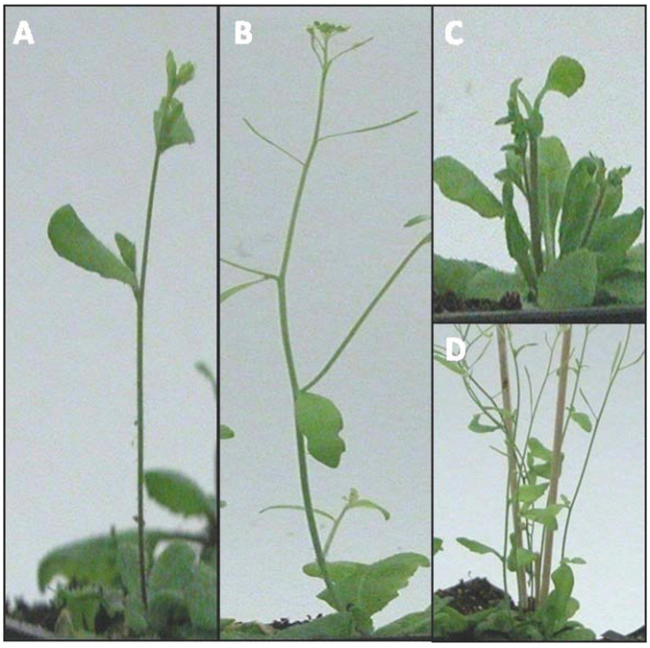

Fig. S1. Examples of altered morphologies observed in RNAi-C HSP90-reduced plants. Plants were grown in long days (16 h light/8 h dark) until flowering. Single inflorescences were observed in WT (*A*) and RNAi-C line 41 (*B*). Multiple inflorescences were observed in lines 83 (*C*) and 19 (*D*).

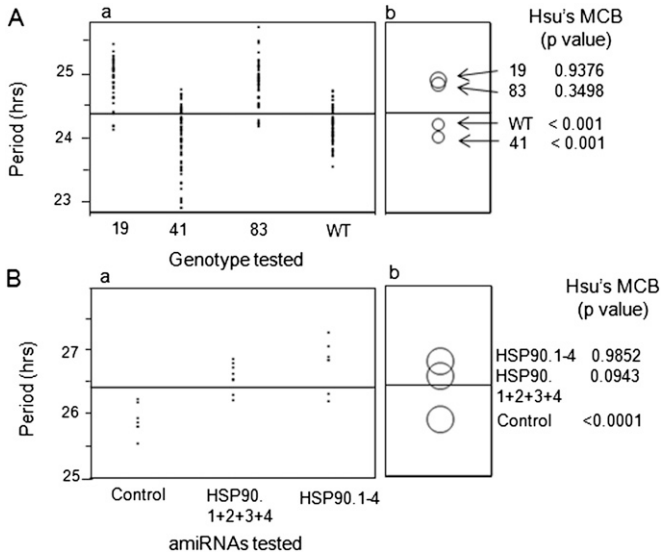

Fig. S2. Scatter plots of individual periods from RNAi and amiRNA trials. (*A*) Individual period values of each of four lines (RNAi-C and WT) from fast Fourier transform nonlinear least squares (FFT-NLLS) analyses are plotted in *a*. The *x* axis indicates the lines tested, and the *y* axis is the period range, which is shared with *b*. (*B*) Individual period values of each well of protoplasts transfected transiently with the indicated amiRNA plasmids from FFT-NLLS analyses are plotted in *a*. The *x* axis indicates the amiRNA plasmid(s) tested, and the *y* axis is the period range, which is shared with *b*. The diameter of the circles in the vertical direction are the 95% confidence interval of period values in each instance calculated by Hsu's multiple comparison with the best (Hsu's MCB). Corresponding Hsu's MCB results are summarized by *P* value. The *P* value in the analysis represents the probability that the period estimation of each individual line does not significantly overlap with the best one based on family or pooled error rate ($\alpha = 0.05$). The horizontal lines in *A* and *B* indicate the grand mean for each data set.

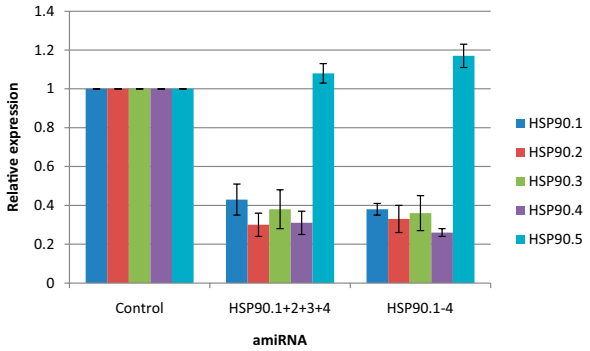

Fig. S3. amiRNA to cytosolic HSP90 reduces expression of the target HSP90 genes. Relative expression of four cytosolic HSP90 and HSP90.5 genes from cDNA of protoplast transfected with control amiRNA, amiR-HSP90.1–4, or amiR-HSP90.1+2+3+4. Protoplast was harvested at ZT 4, after 19 h of incubation after transfection. Expression levels were determined by real-time qPCR and normalized to *ACTIN2* (*ACT2*). Data represent mean ± SEM ($n = 4$).

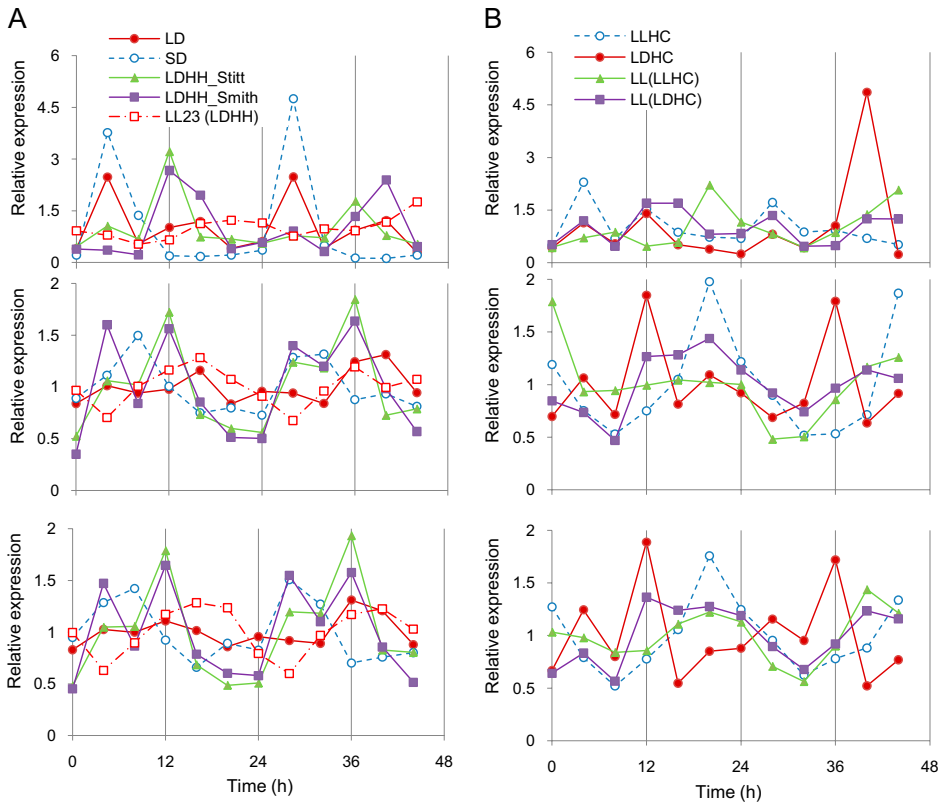

Fig. S4. HSP90 transcript abundance shows rhythmic pattern under diurnal and circadian conditions. (*A*) Transcript abundance of cytosolic HSP90s (HSP90.1–3/4, from the top) under various LD cycles and constant conditions (constant light at 22 °C) after LD entrainment (12 h light/12 h dark). (*B*) Transcriptional abundance under thermo cycles and thermo-photo cycles (HSP90.1–3/4, from the top). LD, 16 h light/8 h dark; SD, 8 h light/16 h dark; LDHH_Smith, 12 h light/12 h dark at 22 °C; LDHH_Stitt, 12 h light/12 h dark at 22 °C; LL23 (LDHH), LL after entrainment to 12 h light/12 h dark; LLHC, constant light, 12 h at 22 °C/12 h at 12 °C; LDHC, 12 h in light at 22 °C/12 h in dark at 12 °C; LL(LLHC), constant condition after LLHC entrainment; LL(LDHC), constant condition after LDHC entrainment. Data are obtained from DIURNAL (http://diurnal.cgrb.oregonstate.edu), and each experiment is normalized to the average value to facilitate comparisons from the various temporal patterns. Experimental details and further explication of the legend can be found at http://diurnal.cgrb.oregonstate.edu.

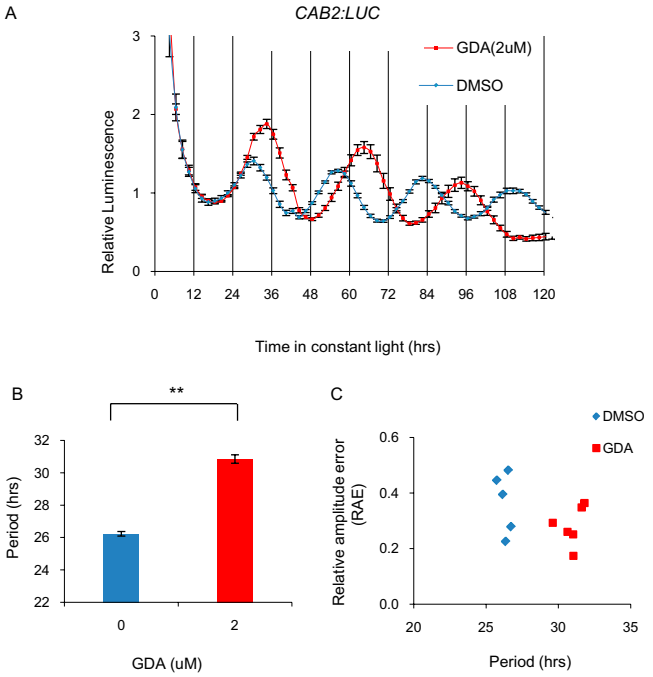

Fig. S5. Reduction in HSP90 lengthens period of the *ztl* null mutant. (*A*–*C*) *ztl-3* seedlings were grown in 12 h light/12 h dark cycles (LD) and released into constant red light as described in Fig. 1 and imaged for *CAB2:LUC* activity. Seedlings were treated with 2 μM GDA or vehicle (DMSO) just before imaging as described in SI Materials and Methods. (*A*) Average luminescence rhythm during imaging with GDA or vehicle treatment. (*B*) Average period values between the treatments ($n = 6$). $^{**}P < 0.01$ (one-way ANOVA), ±SEM. (*C*) Scatter plot comparing circadian periods of the two treatments with relative amplitude error as determined by FFT-NLLS (1). All data are representative of two independent trials.

1. Plautz JD, et al. (1997) Quantitative analysis of *Drosophila* period gene transcription in living animals. *J Biol Rhythms* 12:204–217.

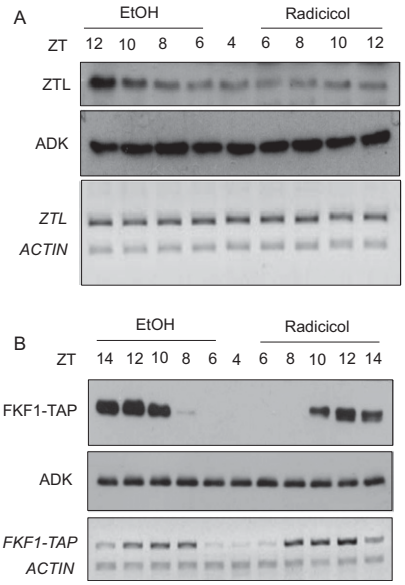

Fig. S6. Radicicol acts posttranscriptionally to diminish ZTL and FKF1 levels. (*A* and *B*) Seedlings were grown 7–10 d in 12 h light/12 h dark (LD) cycles then treated at ZT 4 with 26 μM radicicol or vehicle (EtOH) and sampled every 2 h at the indicated times over an LD cycle. Lights on at ZT 0 and lights off at ZT 12 in all experiments. (*A*) Effects of radicicol on ZTL accumulation. (*B*) Effects of radicicol on FKF1-TAP accumulation. The previously described *FKF1:FKF1-TAP* expressing line was used in these trials and FKF1-TAP detected as previously reported (1). Immunoblots representative of at least two trials. Adenosine kinase (ADK) was used as a loading control for immunoblots; *ACTIN* as a loading control for RT-PCR.

1. Imaizumi T, Tran HG, Swartz TE, Briggs WR, Kay SA (2003) FKF1 is essential for photoperiodic-specific light signalling in *Arabidopsis*. *Nature* 426:302–306.

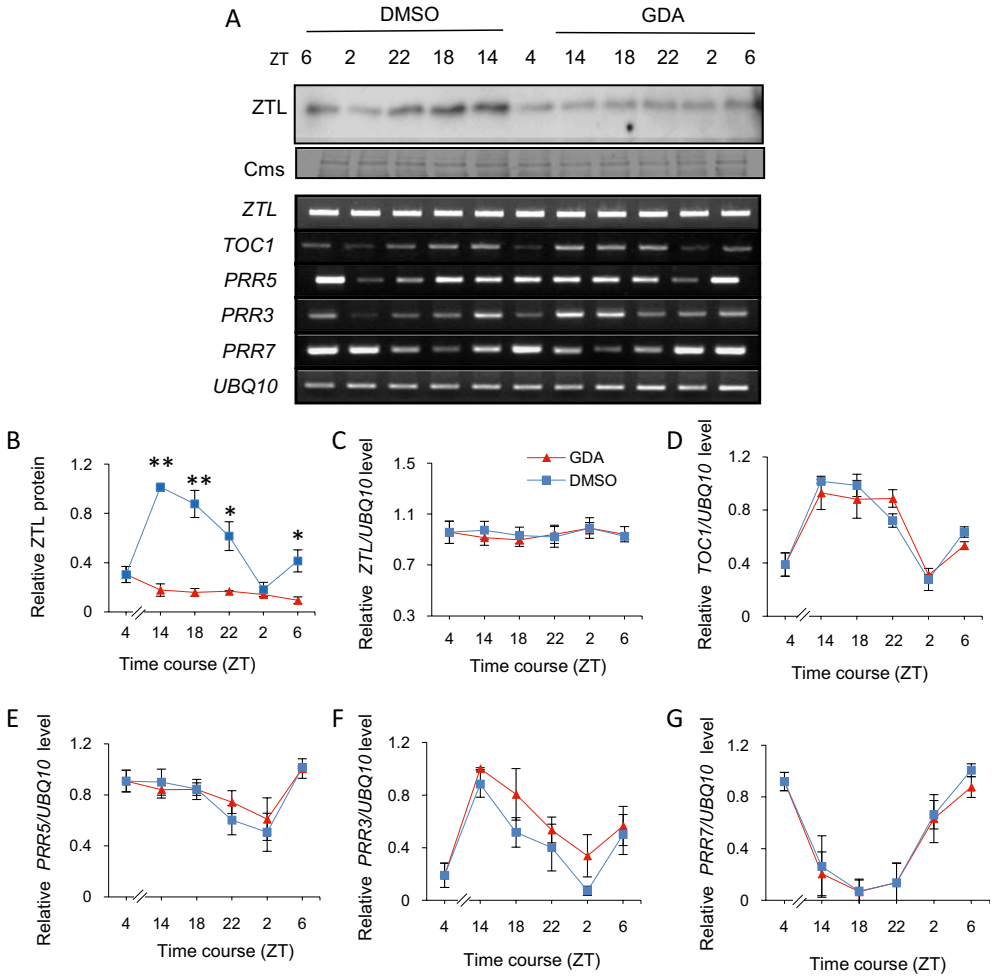

Fig. S7. GDA acts posttranscriptionally to control ZTL levels. (*A*) Diurnal (LD) time course of ZTL protein (*Upper*) and mRNA level of *ZTL*, *TOC1*, *PRR5*, *PRR3*, *PRR7*, and *UBQ10* (from top, *Lower*) under DMSO or GDA treatment. (*B*) Quantification of ZTL protein level. (*C*) Quantification of *ZTL* mRNA level. (*D*) Quantification of *TOC1* mRNA level. (*E*) Quantification of *PRR5* mRNA level. (*F*) Quantification of *PRR3* mRNA level. (*G*) Quantification of *PRR7* mRNA level. All blots are the representative of each set of trials; blue lines with filled square represent mean protein or mRNA level under DMSO treatment; red lines with filled diamonds represent mean protein or mRNA level under GDA; protein levels shown are relative to Coomassie staining (Cms); mRNA levels shown are relative to mRNA level of *UBQ10* at each time point; values were normalized to highest protein or mRNA level. *$0.01 < P \leq 0.05$; **$P \leq 0.01$. Mean is derived from at least three trials; error bars represent ±SEM.

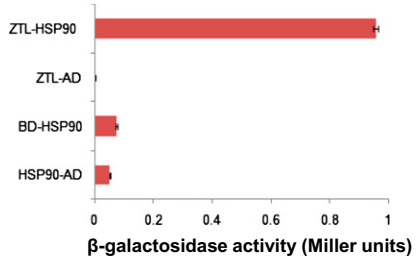

Fig. S8. Interaction between HSP90 and ZTL using yeast two-hybrid analysis. Protein–protein interaction using ZTL-AD and BD-HSP90 plasmids was confirmed by β-galactosidase activity as described in SI Materials and Methods. These results are representative of two independent trials. Error bars indicate ±SEM ($n = 3$).

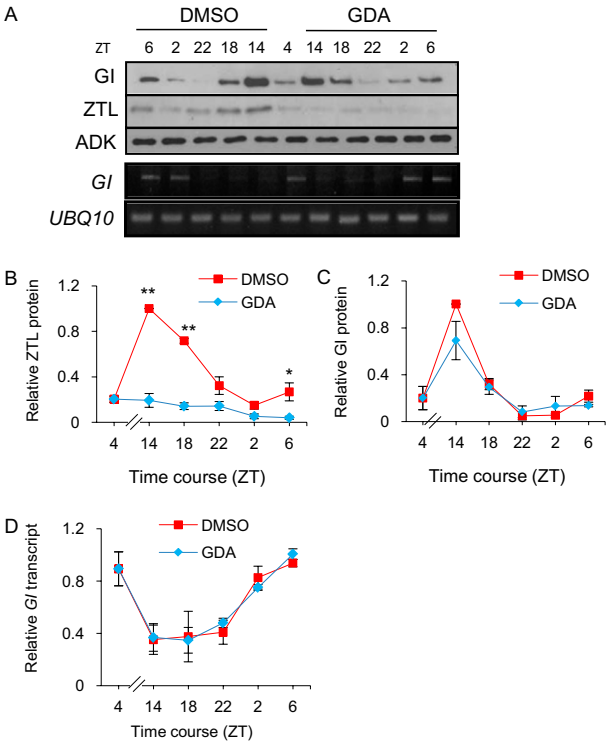

Fig. S9. Suppression of HSP90 does not affect GI accumulation. Seedlings expressing *GI:GI-TAP* were grown 7–10 d in LD cycles then treated at ZT 4 with 5 μM GDA or vehicle (DMSO) and further treated and processed as described in Fig. 2 (main text). (*A*) *Top and Upper Middle*: LD time course of ZTL and GI protein abundance from seedlings subject to the indicated treatment were subjected to GDA or vehicle (DMSO) treatment as described in Fig. 2 (main text). *Bottom*: RNA levels of *GI* expression from the same tissue and time points. (*B*) Quantitation of ZTL levels from *A*. (*C*) Quantitation of GI levels from A. (*D*) Quantitation of *GI* mRNA levels from *A*. *0.01 < p 0.05; **$P \leq 0.01$. All results are the mean of at least three trials; error bars represent ±SEM. All blots are the representative of each set of trials; protein and mRNA levels shown are relative to adenosine kinase (ADK) and UBQ10, respectively and normalized to highest expression level within each time series.

Table S1. Summary of the effects of HSP90 knockdown approaches on circadian period: GDA treatment

Line used	GDA concentration (uM)	*n*	Mean	SEM	*P* Value (one-way ANOVA)
CCA1:LUC	0	12	24.9	0.10	<0.001
CCA1:LUC	2	12	25.6	0.07	
LHY:LUC	0	12	24.9	0.13	0.002
LHY:LUC	2	12	25.5	0.12	

Three to five GDA- treated seedlings (or DMSO-treated controls) were placed into 24-well plates and each well imaged as a pooled group (n = 12).

Table S2. Summary of the effects of HSP90 knockdown approaches on circadian period: Stable RNAi

Line used	RNAi target	*n*	Mean	SEM	*P* value (MCB)
CCR2:LUC	None	71	24.1	0.04	<0.001
41	Cytosolic HSP90	74	23.9	0.04	<0.001
19	Cytosolic HSP90	46	24.8	0.06	0.9376
83	Cytosolic HSP90	52	24.8	0.05	0.3498

Line RNAi-C was crossed to *CCR2:LUC* and three segregants identified. Individual seedlings were assayed in constant red light. MCB, multiple comparisons with the best.

Table S3. Summary of HSP90 amiRNA core sequences and relationships to potential target gene(s)

amiRNA	amiRNA core sequence (5′→3′)	amiRNA source*	Potential target gene(s)	Target recognition sequence (3′→5′)[†,‡]	Hybridization energy (kcal/mol)[§]	Perfect-match-dG cutoff (70%)[¶] (%)
amiR-HSP90.1–4	TTAGAAAGCAGCGT ACTCTTC	W2	*HSP90.1*	GTAGAAAGCAGCATACTCTTC	−40.06	94.04
			HSP90.2	GTAGAAAGCAGCGTACTCCTC	−41.76	98.03
			HSP90.3	GTAGAAAGCAGCGTACTCCTC	−41.76	98.03
			HSP90.4	GTAGAAAGCAGCGTACTCCTC	−41.76	98.03
			HSP90.5	GTAGAACTCATTGTACTCTCC	−25.58	60.05
			HSP90.6	GTAAAACTCATTGTATTCTGC	−12.34	28.97
			HSP90.7	GTAGAATTTAGTGTACTCTTC	−23.07	54.15
amiR-HSP90.1	GATTAAGTAGTCACAAT GTTCGAGATT	A	*HSP90.1*	CTAGAAGTAGTCACAATGTTCAAGTAA	−38.60	75.33
			HSP90.2	TCAG——AG-AAATATCTTCACAACA	−14.75	28.79
			HSP90.3	TCAG——AGAAAAAATCTTCACGA-A	−13.86	27.05
			HSP90.4	TCAG——AG-AAAAAGCTTCAAGATA	−14.71	28.71
			HSP90.5	TGGATAAATCTCGTTCACGCGTGATTT	−13.50	26.35
			HSP90.6	CAATCAATTATTAATCTCTC-CAACAT	−14.65	28.59
			HSP90.7	ACATAATCCATCAAAAAACTGCTTAATT	−12.70	24.79
amiR-HSP90.2	ACATTACCTTTCACA AATCCGAGCTAC	A	*HSP90.2*	ACAATACCTTTCACAAATCCGAGGTAC	−44.28	79.81
			HSP90.1	ACAACACCTTTCACAAAGCTGAGGTAC	−31.22	56.27
			HSP90.3	ACAATACCCTTGACAAACCCAAGGTAC	−33.95	61.19
			HSP90.4	ACGATACCCTTGACAAACCCAAGGTAA	−29.57	53.30
			HSP90.5	ACAACTCCCTTCACAAAGCTCAGATAT	−24.33	43.85
			HSP90.6	ACAACACCTTTAACAAAGCTCAAGTAC	−25.37	45.73
			HSP90.7	ACAAGACCCTTCAAGAAACTCAAATAC	−22.31	40.21
amiR-HSP90.3	TCTCCCGAAAGTGTTG GGGTC	W2	*HSP90.3*	GCTCCCGAAAGTGTTGGGCTC	−42.59	85.69
			HSP90.1	AGCAGCAAAAGTGTTCGGTTC	−20.56	44.34
			HSP90.2	GCTTCCGAAAGTGTTTGGCTC	−27.67	55.67
			HSP90.4	GCTTCCAAAAGTGTTGGGCTC	−32.71	65.81
			HSP90.5	GTTCCCGAGCTCGGCCGGGCT	−25.70	43.85
			HSP90.6	CCCACCCAGCTCTGCTGGATT	−19.84	45.73
			HSP90.7	GGCAGCAAAGTCTTTTGGGTC	−17.20	40.21
amiR-HSP90.4	GGTTACCGTGAAAGAT CCACGCGCCTG	A	*HSP90.4*	GGTCACCGTGAAAGATCCACCGGCCTG	−55.26	84.90
			HSP90.1	AGTGACAGTGAAGGAACCACCAGCTTG	−24.74	38.01
			HSP90.2	GGTCACAGTGAAAGATCCCCCGGCCTG	−47.30	72.67
			HSP90.3	GGTGACGGTGAAAGATCCACCGGCCTG	−43.66	67.08
			HSP90.5	TCTGATCAGATACGAGCTACTATCGGCAAC	N.A.	N.A.
			HSP90.6	CTGAATGGTAAAACTGCTTGAATTTGCTTC	N.A.	N.A.
			HSP90.7	GGAAACAGCAAATTTAC—CGTTAGCCTT	N.A.	N.A.

N.A., not applicable.

*A, From ABRC; W2, Designed using the WMD2 (Web microRNA designer2).

[†]Matched sequences between amiRNA and target sequence are underlined.

[‡]Recognition region of the best candidate target of amiRNA was found using the WMD2 program, and that of other genes was chosen with their homologous region to the recognition region of the best candidate target.

[§]Hybridization of amiRNA to its mRNA target site was calculated using the RNAcofold program in the WMD2 Web site.

[¶]Ratio of the hybridization energy between amiRNA and its target to that between amiRNA and its perfect reverse complement in percent.

Table S4. Summary of the effects of HSP90 knockdown approaches on circadian period: Transient amiRNA

amiRNA transfected	amiRNA target(s)	*n*	Mean	SEM	*P* value (MCB)
Control	None	8	25.9	0.08	<0.0001
One construct	Cytosolic HSP90s	8	26.9	0.10	0.9852
Four constructs	Individual cytosolic HSP90s	8	26.6	0.07	0.0943

Transient transfection of *CCA1:LUC* alone (no construct) or *CCA1:LUC* plus one amiRNA plasmid targeting the four cytosolic HSP90 genes, or plus four amiRNA plasmids targeting four individual genes. Pools of protoplasts of each type were assayed in microtitre wells (n = 8). MCB, multiple comparisons with the best.

Table S5. Summary of primers used for semiquantitative RT-PCR and qPCR-based assessment of HSP90 expression in protoplasts and primers used for amiRNA constructs

Primer name	Sequences (5′ to 3′)	Purpose
HSP90.1-RT-F	AAGACGCTCTCAATTATTGACAGTGG	Real-time RT-PCR
HSP90.1-RT-R	TCGCAATGGTTCCCAAGTTG	Real-time RT-PCR
HSP90.2-RT-F	ATTGGCATGACCAAGGCTGATTTG	Real-time RT-PCR
HSP90.2-RT-R	TGCTTCCATGAATTCCTTGGTTCC	Real-time RT-PCR
HSP90.3-RT-F	TTGGGATGACCAAGGCTGATCTGG	Real-time RT-PCR
HSP90.3-RT-R	AACATCAGCTCCAGCAGCCAAC	Real-time RT-PCR
HSP90.4-RT-F	TGGGATGACCAAGGCTGATTTG	Real-time RT-PCR
HSP90.4-RT-R	CAGCCAATGCCTCCATGAACTC	Real-time RT-PCR
HSP90.5-RT-F	TTCGGGTGGTCAGCTAATATGG	Real-time RT-PCR
HSP90.5-RT-R	TCATGAACTCCAGGCTTGAAGTG	Real-time RT-PCR
ACT2-RT-F	CAGTGTCTGGATCGGAGGAT	Real-time RT-PCR
ACT2-RT-R	TGAACAATCGATGGACCTGA	Real-time RT-PCR
FKF1-F	ACAGCTCGTGCACCATTGAG	RT-PCR
FKF1-R	TCCAAAGATGATGACCCTAC	RT-PCR
HSP90.1–4_I miR-s	gaTTAGAAAGCAGCGTACTCTTCtctctcttttgtattcc	amiRNA constructs
HSP90.1–4_II miR-a	gaGAAGAGTACGCTGCTTTCTAAtcaaagagaatcaatga	amiRNA constructs
HSP90.1–4_III miR*s	gaGACGAGTACGCTGGTTTCTATtcacaggtcgtgatatg	amiRNA constructs
HSP90.1–4_IV miR*a	gaATAGAAACCAGCGTACTCGTCtctacatatatattcct	amiRNA constructs
HSP90.3_I miR-s	gaTCTCCCGAAAGTGTTGGGGTCtctctcttttgtattcc	amiRNA constructs
HSP90.3_ II miR-a	gaGACCCCAACACTTTCGGGAGAtcaaagagaatcaatga	amiRNA constructs
HSP90.3 _III miR*s	gaGAACCCAACACTTACGGGAGTtcacaggtcgtgatatg	amiRNA constructs
HSP90.3 _IV miR*a	gaACTCCCGTAAGTGTTGGGTTCtctacatatatattcct	amiRNA constructs

See http://wmd.weigelworld.org/cgi-bin/mirnatools.pl for details of design principles and nomenclature.